Published online: March 30, 2019

Original Research

Cerebral cortex functional networks of magnetic stimulation at acupoints along the pericardium meridian

Yang-yang Dai[1,2], Ning Yin[1,2,*], Hongli Yu[1,2] and Gui-zhi Xu[1,2]

[1] *State Key Laboratory of Reliability and Intelligence of Electrical Equipment, Hebei University of Technology, Tianjin, 300130, China*

[2] *Key Laboratory of Electromagnetic Field and Electrical Apparatus Reliability of Hebei Province, Hebei University of Technology, Tianjin, 300130, China*

*Correspondence: yinning@hebut.edu.cn (Ning Yin)

DOI: 10.31083/j.jin.2019.01.126

The coordinated regulating mechanism of magnetic stimulation at acupoints along the pericardium meridian was studied by cerebral cortical functional networks. Electroencephalogram signals of 14 subjects (eight males and six females) were recorded in resting state and following magnetic stimulation at Neiguan and Daling acupoints along the pericardium meridian. The corresponding cortical functional networks were constructed and analyzed by group independent component analysis, standard low-resolution brain electromagnetic tomography, short-time Fourier transform, and complex network theory. Results showed that during magnetic stimulation at Daling and Neiguan acupoints, the functional connections of the nodes in the brain areas associated with movement respectively decreased by 7.3% and 19.9%, and the functional connections of the nodes in brain areas associated with advanced cognitive functions such as emotion, memory and language respectively increased by 24.9% and 18.8%. Changes of topological structure were similarly related to the efficacy of acupoints along the pericardium meridian. Magnetic stimulation also caused different topological changes consistent with the therapeutic function of specific acupoint. This study provided new evidence revealing mechanisms of brain functional integration and network synergy in the acupoint stimulation pathway.

Keywords

Acupuncture; pericardium meridian; acupoint; magnetic stimulation; cerebral cortex functional network

1. Introduction

Acupuncture is widely used in the rehabilitation of various diseases (Chen et al., 2016; Tao and Ma, 2016). The effect of clinical treatment by acupuncture is obvious. However, the mechanism of acupuncture has no explaination based on modern biology and medical science. Traditional acupuncture depends on the experience of the physician and is difficult to quantify (Sun et al., 2014; Guo et al., 2015). Magnetic stimulation is noninvasive and widely recognized in the rehabilitation of neurological disease. The combination of magnetic stimulation and traditional acupoint theory helps to achieve a quantifiable international technical standard (Yin et al., 2013). Currently, magnetic stimulation at acupoints has been applied to treat diseases such as depression (Xiong et al., 2018).

According to modern medical theory, the brain is the material basis of all functional activities of organism. The brain network makes it possible to reveal the acupuncture mechanism of brain functional integration (Cai et al., 2018). It is found that the topological structure of brain network established by the electrode positions directly as network nodes changes during magnetic stimulation at acupoints (Yin et al., 2013; Guo et al., 2017; Xing et al., 2016). It is unclear whether there is a correspondence between the functional network connectivity of the cerebral cortex and the function of specific acupoints.

The acupoints along the pericardium meridian can usually be used to calm the mind and treat mental diseases in clinic (Han et al., 2014). Neiguan (PC6) and Daling (PC7) are two acupoints along the pericardium meridian. PC6 can be used to treat diseases such as senile dementia, depression, and insomnia (Lu et al., 2014; Fu et al., 2005; Xia et al., 2012). PC7 is often used to treat affective disorders such as, cognitive disorders, and insomnia (Yuan et al., 2003; Hua et al., 2012; Zhang and Gu, 2011). Here, PC6 and PC7 were selected as stimulus targets and electroencephalogram (EEG) signals were recorded. Group independent component analysis (Group ICA), standard low-resolution brain electromagnetic tomography (sLORETA) (Pascual-Marqui, 2002), and graph theory were combined to construct cortical functional network (Xia et al., 2013). Brain integration in the stimulation pathway was analyzed from the perspective of the complex network. It helped in revealing the intrinsic interaction mechanism of "acupoint-brain-organ", and provided new evidence for the regulating mechanism of acupoint stimulation.

2. Materials and Methods

2.1. Subjects

Healthy right-handed subjects (eight males and six females) aged 21 to 25 years old without history of mental illness were re-

Journal of Integrative Neuroscience

cruited. The experiment was approved by the Biomedical Ethics Committee of Hebei University of Technology (approval number HEBUThMEC2018005). No ethical issues were involved and the study conformed to the Helsinki Declaration. Experimental methods and operations were consistent with approved guidelines. All subjects signed informed consent before the experiment.

2.2. Acupoint selection

Left-hand PC6 and PC7 acupoints along the pericardium meridian were selected as stimulus targets, as shown in Fig. 1. PC6 and PC7 are between the palmaris longus tendon and the carpal flexor tendon of the radial side. PC6 is located on the volar side of the forearm, five centimeters above the carpal transverse stripe. PC7 is located at the midpoint of the carpal palmar transverse stripe.

2.3. Experiment

Magstim Rapid^2 repetitive pulse magnetic stimulator (Magstim company, UK) with an "8" shaped coil (model number 9925-00) was used for repetitive stimulation. The coil was placed approximately 0.5 cm above the skin, and the focus center was directly opposite the acupoint. Stimulation intensity was set to 80% of the maximum output intensity (2.2 Tesla) and the stimulation frequency was one Hertz. EEG signals were recorded (NeuroScan Company, USA) at a sampling frequency of 1000 Hz using 64 Ag-AgCl electrodes placed according to the international 10-20 system.

Subjects sat eyes closed with earplugs inserted. The experiment flowchart is given in Fig. 2. The main steps were:

(1) Resting state EEG recorded for 60 seconds.

(2) EEG signals recorded for 60 seconds as PC7 stimulated.

(3) Subjects rested for 60 minutes.

(4) EEG signals recorded for 60 seconds as PC6 stimulated.

EEG signals were pre-processed to remove interference prior to construction of the cortical functional network. EEG data was preprocessed off-line by 0.5-40 Hz band-pass filtering, artifact removal, abnormal segments elimination, converting data to average reference, segmentation, and baseline correction.

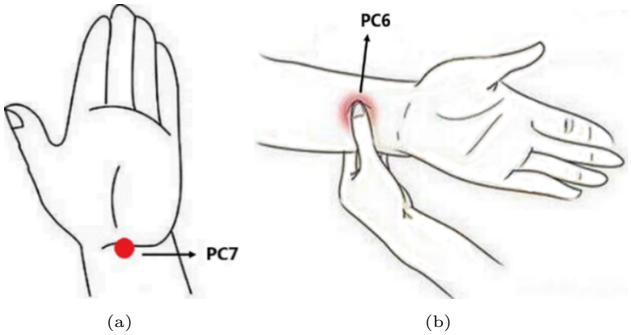

Figure 1. Position of acupoints. (a) PC7. It is located at the midpoint of the carpal palmar transverse stripe. (b) PC6. It is located five centimeters above the midpoint of the carpal palmar transverse stripe.

2.4. Group ICA

Group ICA was employed to separate source signals from the mixed EEG data of multiple subjects. Row-wise Group ICA (Schmithorst and Holland, 2004) is suited for analysis of brain area activation when subjects are in a single specific stimulation state.

The mathematical model is:

$$[X_1, X_2, \ldots, X_n] = A\,[S_1, S_2, \ldots, S_n], \tag{1}$$

where X_n is a $K \times V$ matrix, which represents the EEG data of subject N. K gives the number of electrodes, and V gives the number of time points.

2.5. Source localization

sLORETA is a method of source localization employed to reconstruct the current density of the cerebral cortex (Chen et al., 2013; Yang et al., 2015; Li et al., 2017). The relationship between EEG signals on the scalp and sources on the cortex can be expressed as:

$$\varphi = KJ, \tag{2}$$

where φ represents the EEG signals, K is a $m \times n$ $(n \gg m)$ matrix of forward model coefficients, and J is a $n \times l$ matrix that represents the current density of signal sources.

Eq. (2) can be uniquely solved by zero-order Tikhonov-Philips regularization. The cost function is:

$$F = \|\varphi - KJ\|^2 + \alpha \|J\|^2, \tag{3}$$

where α is the regularization parameter and $\alpha \geq 0$.

To solve for J, the given values of K, φ, and α are inserted into Eq. (3) and the minimum cost function is taken:

$$\hat{J} = T\varphi, \tag{4}$$

where $T = K^T \left[KK^T + \alpha H\right]^+$, $H = \boldsymbol{I} - II^T / I^T I$, $\boldsymbol{I}$ is the identity matrix, and I is the unit vector.

2.6. Construction of cerebral cortex functional network

First, Group ICA was employed to analyze preprocessed EEG data. Components related to brain activity were then selected to reconstruct EEG data. The current density distribution of the cerebral cortex was calculated by sLORETA based on the reconstructed EEG data. Areas with the maximum current density were considered to be network nodes (Chen et al., 2013; Yang et al., 2015). The relationship between the nodes was given by the cross-correlation coefficients of the alpha-band power spectrum (Chen et al., 2013).

Second, a short-time Fourier transform was calculated to obtain power spectrums of the selected EEG components. The cross-correlation coefficient matrix was calculated based on a cross-correlation analysis. To improve the normality of the data, a Fisher Z transform was performed on the cross-correlation matrix. Any significant differences between the cross-correlation coefficients and zero were then assessed by two-sided one-sample t-test, and a false discovery rate (FDR) correction was applied to multiple test results (Salvador, 2005).

Subsequently, binary matrices were generated. If the element

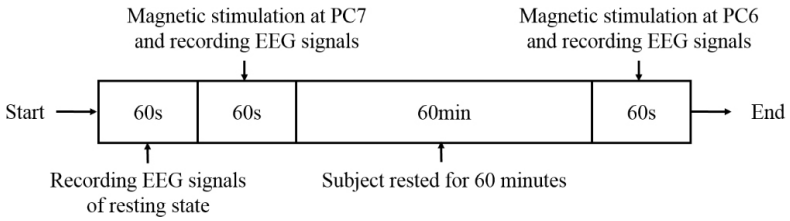

Figure 2. Schematic diagram of experiment time line. EEG signals of resting state, stimulation at PC7 and PC6 respectively recorded for 60 seconds.

in the matrix was one, it corresponded to the cross-correlation coefficients with statistically significant results ($p < 0.05$, FDR corrected). Finally, network connection edges were generated according to the binary matrix.

2.7. Parameters of the functional brain network

The degree of a node refers to the number of edges directly connected to a given node. It reflects the importance of the node in the network. The mean degree is given by:

$$D = \frac{1}{N}\sum_{i=1}^{N} D_i, \tag{5}$$

where N is the number of nodes and D_i is the degree of the ith node.

3. Results

The source localization of EEG data reconstructed by the component related to brain activity is shown as Fig. 3. In this figure the corresponding current density distribution in the cerebral cortex of the reconstructed EEG signals was estimated and the Montreal Neurological Institute 152 brain template coordinate of the maximum current density position in the three-dimensional cerebral cortex at five millimeters resolution was given. On the color bar, the + and − preceeding each number indicates current flow direction. Moving from the middle of the color bar to either side the current density gradually increases.

The binary matrix is given in Fig. 4. The abscissa and ordinate represented the serial number of nodes. White represented one, and black represented zero. If an element in the matrix was 1, there was a connection edge between the corresponding nodes. Fig. 4(a), Figure 4(b) and Fig. 4(c) give the binary matrices of the resting state and magnetic stimulation at PC7 and PC6, respectively.

The alpha-wave cortical cerebral functional network is illustrated from the sagittal, axial, and coronal directions in Fig. 5. The small red spheres give the node locations of the functional network. Labels of the network nodes indicate cortical Broadmann Areas (BA) (Brodmann, 1909; Garey, 2006). Blue lines give the connection edges between network nodes. Fig. 5(a), Fig. 5(b), and Fig. 5(c) illustrate the functional network of the resting state and magnetic stimulation at PC7 and PC6, respectively.

The node number and mean node degree of each Brodmann Area is shown in Fig. 6. The changes in the number of nodes for each BA of the resting state and the magnetic stimulation at PC7 and PC6 are indicated in Fig. 6(a) by a dotted line with a circle, square, and triangle, respectively. In Fig. 6(b), white, gray, and black histograms are used to show changes in the mean degree of nodes at each BA of the resting state, and magnetic stimulation at PC7 and PC6, respectively.

BA1, BA2, BA3, BA5 and BA7 in Fig. 6 are brain areas related to somatic sensation. BA4 is the main source of motor activation. BA6 and BA8 comprise anterior motor cortex. BA18 and BA19 are areas associated with vision. BA9, BA10, BA11, BA21, BA38, BA39, BA40, BA45, BA46, and BA47 are related to advanced cognitive functions. BA9, BA10, and BA11 are closely related to functions such as emotion and memory. BA38 participates in the processes of behavior, affection, and decision. BA46 is concerned with maintaining attention and managing working memory. BA21, BA39, BA40, BA45 and BA47 are involved with processing and expression of language.

In the brain areas related to somatic sensation the mean degree and number of nodes in BA1 and BA7 increased, the nodes in BA2 disappeared, the mean degree in BA3 decreased, and the mean degree in BA5 increased during stimulation at PC7 compared with the resting state. In brain areas associated with movement the mean degree in BA6 increased but the number of nodes decreased, the mean degree and the number of nodes in BA8 both decreased, and the mean degree and number of nodes in BA4 both increased. In visually-related areas the mean degree in BA18 decreased but the number of nodes increased. Conversely, in BA19 the mean degree of nodes increased but the number of nodes decreased. In areas associated with advanced cognitive function the mean degree in BA9 and BA45 increased, the mean degree in BA10, BA21, and BA47 decreased, and the mean degree in BA11 increased but the number of nodes decreased, BA38 was activated and the mean degree and the number of nodes in BA39 and BA40 both increased.

During stimulation at PC6 the nodes in BA1 and BA2 disappeared, the mean degree in BA3 increased, and the mean degree and the number of nodes in BA5 and BA7 increased comparing with the resting state. There were no nodes in BA4. The mean degree in BA6 increased but the number of nodes decreased. The mean degree of nodes in BA8 increased. The mean degree and number of nodes in BA18 increased, as did the mean degree in BA19. The mean degree and the number of nodes in BA9 and BA47 both increased. The mean degree in BA10, BA39, BA40, BA45, and BA46 increased. The mean degree in BA11 increased but the number of nodes decreased. The mean degree and number of nodes in BA21 both decreased.

The number of nodes and the mean degree are combined to reflect changes of functional connectivity in each Brodmann Area. Usually, multiple Brodmann Areas are responsible for a specific brain function. If the change trend of the two indicators is consis-

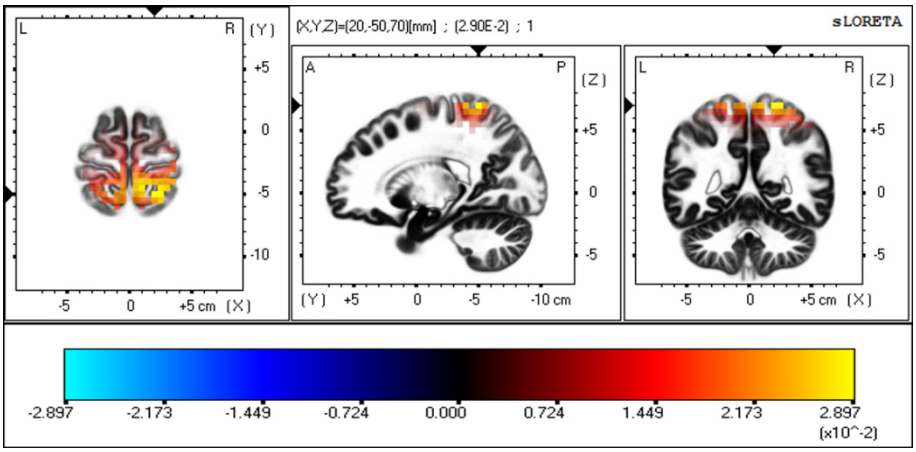

Figure 3. Source localization of the EEG component. It gives the results of source localization from three directions. The current density gradually increases from the middle of the color bar to either side.

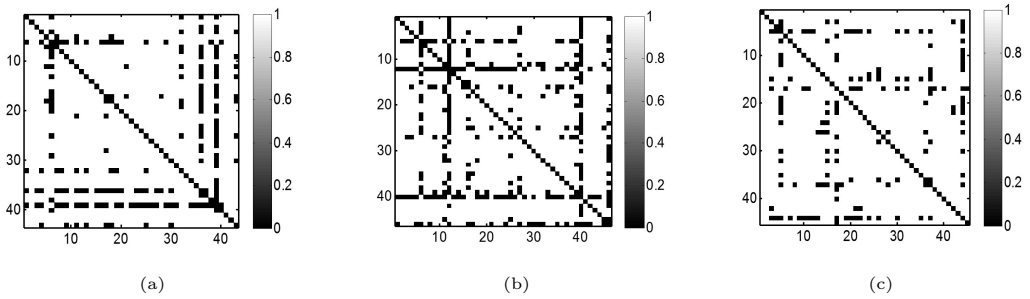

Figure 4. The binary matrix (a) Resting state. (b) Stimulation at PC7. (c) Stimulation at PC6. The abscissa and ordinate represent the serial number of nodes. White represents the element in the matrix is 1, and black represents 0.

tent in all Brodmann Areas, the changes in functional connectivity of specific nodes in the specific functional areas can be approximately estimated. Otherwise, in-depth analysis is required.

The number of connections in specific functional areas is given in Table 1, where "-" indicates absence of network nodes in the given area in the corresponding state. From data in Table 1, the calculated functional connectivity related to somatic sensation generally increased by 26.0% and 21.2% during the stimulation at PC7 and PC6, respectively, compared with the resting state. The functional connections associated with movement decreased by 19.9% and 7.3% during stimulation at PC6 and PC7, respectively. The functional connections associated with vision increased by 37.9% and 3.9% during the stimulation at PC6 and PC7, respectively. The functional connections of the nodes in brain areas associated with advanced cognitive functions during magnetic stimulation at PC7 and PC6 increased by 24.9% and 18.8%, respectively.

4. Discussion

The pericardium meridian has an important influence on human cognitive activity and spiritual consciousness. Acupoints along the pericardium meridian can be used to treat mentally related disease (Yu et al., 2016; Zhang et al., 2012; Hua et al., 2012). For example, PC6 can be used to treat diseases such as senile dementia, depression, and insomnia (Lu et al., 2014; Fu et al., 2005; Xia et al., 2012). PC7 is often used to treat affective disorders, cognitive disorders, and insomnia (Yuan et al., 2003; Hua et al., 2012; Zhang and Gu, 2011). These diseases seriously affect emotion, memory, language, and other advanced cognitive functions. Results show that during magnetic stimulation at PC6 and PC7 functional connectivity of brain areas related to advanced cognitive functions such as emotion, memory, and language increased by 18.8% and 24.9%, respectively. This suggested that advanced cognitive functions were somewhat promoted in the condition of stimulation at PC6 and PC7 along the pericardium meridian (Zhao, 2008; Fu et al., 2005). When stimulating PC7 and PC6, the functional connections of the nodes in the brain areas associated with movement decreased by 19.9% and 7.3%, respectively, compared to the resting state. This indicated that motor function of brain areas was restrained to a certain extent. This is conducive to the maintainence of quiet or calm, making it easier for people to calm the mind and stabilize the spirit (Han et al., 2014).

The functional connectivity of the nodes in brain areas related to somatic sensation increased by 21.2% and 26.0% during stimulation at PC6 and PC7, respectively. It was speculated that somatosensory cortex enhances the integration and modulation of tactile information during magnetic stimulation of acupoints (Ma et al., 2016). It has been reported that the occipital lobe, associated with vision, was activated when stimulating acupoints along the pericardium meridian (Zhou et al., 2014). Here it was found that the functional connectivity of nodes located in visual areas

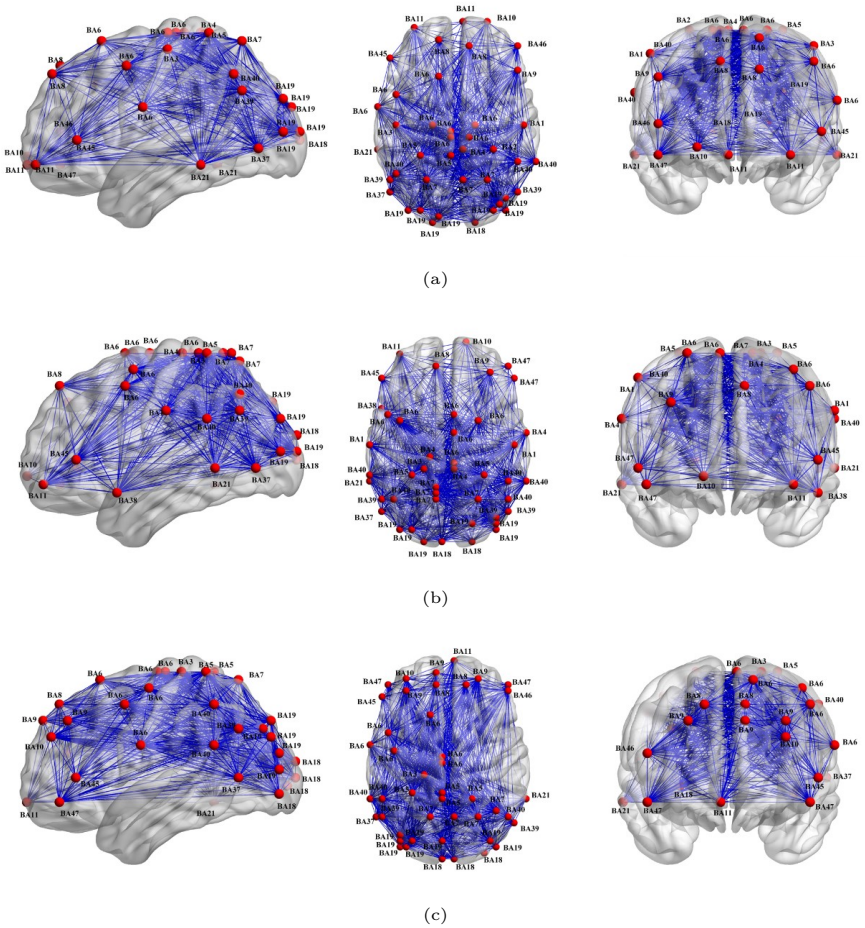

Figure 5. α-wave cortical cerebral functional network. (a) Resting state. (b) Stimulation at PC7. (c) Stimulation at PC6. The columns from left to right represent the sagittal, axial, and coronal directions. The small red spheres and blue lines respectively give the node locations and the connection edges between nodes.

increased by 37.9% and 3.9% during stimulation at PC6 and PC7, respectively. This provides new evidence for the study of the relationship between vision and the acupoint function of the pericardium meridian.

Additional to similarities described above, there were differences in functional brain networks during stimulation at PC6 and PC7 along the pericardium meridian. PC7 was effective in the clinical treatment of affective disorders (Yuan et al., 2003). Results showed that BA38, closely related to emotional processes, was activated only when PC7 was stimulated. This indicated that the effect of stimulation at acupoints along the pericardium meridian was consistent with their specific therapeutic function (Lu and Shan, 2010). Further, some brain areas such as BA18 and BA19, that seem to have no obvious relation to acupoint function, were also activated (Gabrieli et al., 1995; Rosenbaum et al., 2007). This indicated that the brain performed a variety of neural activities through the combination of multiple brain areas (Tu et al., 2013).

Limitations remain with this report. For example, the effect of magnetic stimulation at other acupoints and long-term effects have not been explored. In future work, feature extraction and classification can be performed on functional brain networks, which has the prospect of clinical application in the evaluation of the efficacy of acupoint stimulation therapy. Additionally, the methods of this paper can also be extended to analyze brain networks related to disease, which may be helpful for their diagnosis.

5. Conclusion

Cortical functional networks based on EEG signals in response to magnetic stimulation at PC6 and PC7 along the pericardium meridian were constructed then analyzed by group ICA, sLORETA, and complex network analysis. Results showed that some common brain areas were activated and some similar topological changes of the structure of brain networks were induced by magnetic stimulation at PC6 and PC7. This was basically consistent with the efficacy of acupoints along the pericardium meridian. Specifically, connections related to movement decreased, and the connectivity of nodes located in brain areas associated with advanced cognitive functions, such as emotion, memory, and language, increased during magnetic stimulation. Beyond that, magnetic stimulation at PC6 and PC7 caused some different changes in functional networks, which were related to the specific therapeutic function of acupoints. It was found there was a certain correspondence between cortical functional network connectivity and the function of PC6 and PC7. In summary, this study provides new evidence for the regulatory mechanisms of acupoint stimulation

Table 1. The number of connections in specific functional areas.

Brain function	Resting state	PC7 Magnetic stimulation	PC6 Magnetic stimulation
Somatic sensation	288	363	349
Movement	381	355	305
Vision	309	321	426
Advanced cognition	414	517	492

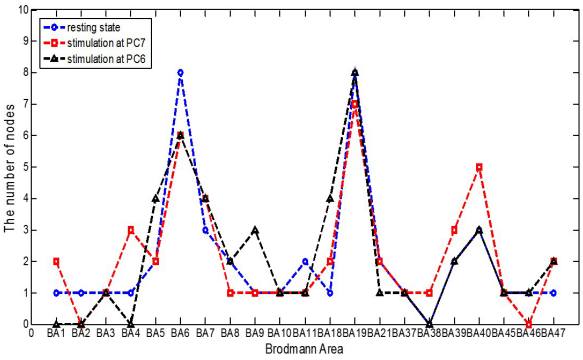

(a)

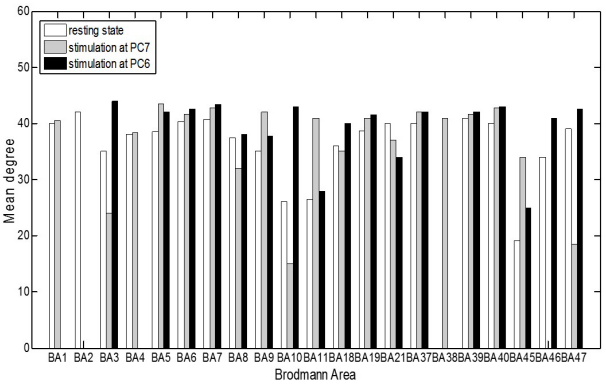

(b)

Figure 6. Number and mean degree of nodes in each Brodmann Area. (a) Number of nodes. A dotted line with circle, square, and triangle respectively indicates the number of nodes in each BA of the resting state and the magnetic stimulation at PC7 and PC6. (b) Mean degree of nodes. White, gray, and black histograms respectively show the mean degree of nodes in each BA of the resting state, and magnetic stimulation at PC7 and PC6.

through cortical functional networks corresponding to the clinical functions of PC6 and PC7 along the pericardium meridian.

Acknowledgments

This work was supported in part by the Natural Science Foundation of China under Grant 51707055, Grant 51877067, Grant 51877068 and Grant 51677053 and in part by the Natural Science Foundation of Hebei Province, China, under Grant E2016202155.

Conflict of Interest

There are no conflicts of interest.

Submitted: December 07, 2018
Accepted: March 26, 2019
Published: March 30, 2019

References

Brodmann, K. (1909). *Vergleichende lokalisationslehre der Großhirnrinde in ihren prinzipien dargestellt auf grund des Zellenbaues*. Leipzig: Verlag von Johann Ambrosius Barth. (In German)

Cai, R. L., Shen, G. M., Wang, H., Guan, Y. Y. (2018) Brain functional connectivity network studies of acupuncture: a systematic review on resting-State fMRI. *Journal of Integrative Medicine* **16**, 26-33.

Chen, J. L., Ros, T., Gruzelier, J. H. (2013) Dynamic changes of ICA-derived EEG functional connectivity in the resting state.*Human Brain Mapping* **34**, 852-868.

Chen, X., Huang, W., Deng, J., Cheng, X. L., Chen, L., Zhou, Z. Y. (2016) Effect of acupuncture therapy on simple obesity in adults: a meta-analysis. *Journal of Clinical Acupuncture and Moxibustion* **32**, 64-69. (In Chinese)

Fu, P., Jia, J. P., Zhu, J., Huang, J. J. (2005) Effects of acupuncture at neiguan (PC6) on human brain functional imaging in different functional states. *Chinese Acupuncture & Moxibustion* **25**, 784-786. (In Chinese)

Gabrieli, J. D., McGlinchey-Berroth, R., Carrillo, M. C., Gluck, M. A., Cermak, L. S., Disterhoft, J. F. (1995) Intact delay-eyeblink classical conditioning in amnesia. *Behavioral Neuroscience* **109**, 819-827.

Garey, L. J. (2006) *Brodmann's localisation in the cerebral cortex*. New York: Springer.

Guo, L., Wang, Y., Yu, H. L., Yin, N., Li, Y. (2015) Brain functional network based on approximate entropy of EEG under magnetic stimulation at acupuncture point. *Transactions of China Electrotechnical Society* **30**, 31-38. (In Chinese)

Guo, L., Chen, Y. G., Wang, Y., Yu, H. L., Xu, G. Z. (2017) Construction and analysis of brain functional vetwork based on C0 complexity under magnetic stimulation at acupoint of neiguan. *Transactions of China Electrotechnical Society* **32**, 155-163. (In Chinese)

Han, H. Y., Zhang, C., Yan, B., Tong, L., Lei, Y., Zhou, H., He Q. (2014) Influence of acupuncture in acupoints of the pericardium meridian on functional connectivity of resting-state posterior cingulate cortex in health people. *Journal of Beijing University of Traditional Chinese Medicine* **37**, 195-198. (In Chinese)

Hua, Y. H., Chen, X. H., Li, Z., Zhang, Y., Lei, X. (2012) Clinical study on effect of Jin needing plus daling point combined with music therapy on mild cognitive dysfunction after stroke. *Chinese Archives of Traditional Chinese Medicine* **30**, 1802-1804. (In Chinese)

Li, J., Chen, G. Z., Chen, C. X. (2017) Research on mental fatigue caused by watching 3DTV based on EEG signal tracing analysis. *Chinese Journal of Biomedical Engineering* **36**, 46-52. (In Chinese)

Lu, N., Shan, B. C. (2010) The Effects of Different Acupoints in the same meridian: a functional magnetic resonance imaging study. *Chinese Journal of Medical Physics* **27**, 1916-1920. (In Chinese)

Lu, J., Jin, S. Y., Bao, W. Y., Hu, L., Liang, J., Tu, Y. (2014) Ef-

fects of acupuncture on astrocytes in prefrontal cortex of chronic stress depression rats. *Journal of Traditional Chinese Medicine* **55**, 1323-1326. (In Chinese)

Ma, N., Wang, X. M., Tian, M., Liu, J., Qi, H. Z., Ming, D., et al. (2016) Research on effects of 20 Hz frequency stomatosensory vibration stimulation on electroencephalogram features. *Journal of Biomedical Engineering* **33**, 1046-1052. (In Chinese)

Pascual-Marqui, R. D. (2002) Standardized low-resolution brain electromagnetic tomography (sLORETA): technical details. *Methods and findings in experimental and clinical pharmacology* **24**, 5-12.

Rosenbaum, R. S., Winocur, G., Grady, C. L., Ziegler, M., Moscovitch, M. (2007) Memory for familiar environments learned in the remote past: fMRI studies of healthy people and an amnesic person with extensive bilateral hippocampal lesions. *Hippocampus* **17**, 1241-1251.

Salvador, R. (2005) Neurophysiological architecture of functional magnetic resonance images of human brain. *Cerebral Cortex* **15**, 1332-1342.

Schmithorst, V. J., Holland, S. K. (2004) Comparison of three methods for generating group statistical inferences from independent component analysis of functional magnetic resonance imaging data. *Journal of Magnetic Resonance Imaging* **19**, 365-368.

Sun, C. Z., Bai, L. J., Niu, X., Chen, H. Y., Chen, P., Zhang, M., et al. (2014) Heterogeneous neural pathways underlying acupuncture revealed by multivariate granger causality analyses. *Chinese Journal of Magnetic Resonance Imaging* **5**, 423-429. (In Chinese)

Tao, X. and Ma, T. M. (2016) Development of researches on acupuncture treatment of peripheral nerve injury. *Acupuncture Research* **41**, 90-93. (In Chinese)

Tu, S., Zhao, G., Cao, X. J., Wang T., Qiu J., Zhang Q. L. (2013) A review on researches of nrain networks. *Advances in Psychology* **3**, 277-283. (In Chinese)

Xia, F. X., Gan, J., Ye, H. M. (2012) Clinical observations on the efficacy of catgut embedding at point neiguan (PC6) plus auricular point plaster therapy in treating insomnia. *Shanghai Journal of Acupuncture and Moxibustion* **31**, 233-235. (In Chinese)

Xia, M., Wang, J., He, Y. (2013) BrainNet viewer: a network visualization tool for human brain connectomics. *PLoS ONE* **8**, e68910.

Xing, Y. Y., Geng, Y. H., Zhang, X., Yu, H. L., Xu, G. Z. (2016) The construction and analysis of brain functional network on the EEG response of magnetic stimulation at guangming point. *Chinese Journal of Biomedical Engineering* **35**, 684-690. (In Chinese)

Xiong, W. W., Li, L., Liu, H. J., Wang, X. C. (2018) Clinical research of traditional Chinese medicine combined with repeated transcranial magnetic stimulation in intervening diabetic depression. *Clinical Journal of Traditional Chinese Medicine* **30**, 713-715. (In Chinese)

Yang, J., Chen, S. S., Huangfu, H. R., Liang, P. P., Zhong, N. (2015) Dynamic functional connectivity of electroencephalogram in the resting state. *Acta Physica Sinica* **64**, 382-391. (In Chinese)

Yin, N., Xu, G. Z., Yu, H. L., Zhou, Q., Guo, L. (2013) Brain functional network influenced by magnetic stimulation at acupoints. *Chinese Journal of Biomedical Engineering* **32**, 184-190. (In Chinese)

Yin, N., Xu, G. Z., Zhou, Q. (2013) Construction and analysis of complex brain functional network under acupoint magnetic stimulation. *Acta Physica Sinica* **62**, 569-576. (In Chinese)

Yu, H. L., Xu, G. Z., Guo, L., Fu, L. D., Yang, S., Shi, S., Lv, H. (2016) Magnetic stimulation at neiguan (PC6) acupoint increases connections between cerebral cortex regions. *Neural Regeneration Research* **11**, 1141-1146.

Yuan, J., Li, M., Su, Z. W., Wang, Y. M. (2003) Control observation on daling (PC7) for treatment of affective disorder after apoplexy. *Chinese Acupuncture & Moxibustion* **23**, 389-390. (In Chinese)

Zhang, G., Yin, H., Zhou, Y. L., Han, H. Y., Wu, Y. H., Xing, W., Xu, H. Z., Zuo, X. N. (2012) Capturing amplitude changes of low-frequency fluctuations in functional magnetic resonance imaging signal: a pilot acupuncture study on neiGuan (PC6). *Journal of Alternative and Complementary Medicine* **18**, 387-393.

Zhang, L. and Gu, F. (2011) Study process of tuina for insomnia in recent 10 years. *Journal of Acupuncture and Tuina Science* **9**, 388-396. (In Chinese)

Zhao, B. X. (2008) Study on the mechanism of acupuncture at daling (PC7) for mental diseases by fMRI. *Chinese Acupuncture & Moxibustion* **28**, 429-432. (In Chinese)

Zhou, Y. L., Xu, H. Z., Duan, Y. L., Zhang, G., Su, C. G., Wu, Y. H., Xing, W., Jin, X. Y. (2014) Effect of acupuncture at pericardium point of amplitude of low frequency fluctuations of healthy people in resting state functional magnetic resonance imaging. *Chinese Journal of Integrated Traditional and Western Medicine* **34**, 1197-1201. (In Chinese)